A Multi-module Microfluidic Platform for Continuous Pre-concentration of Water-soluble Ions and Separation of Oil Droplets from Oil-in-Water (O/W) Emulsions Using a DC-biased AC Electrokinetic Technique

Dhiman Das[1], Dinh Tuan Phan[2], Zhao Yugang[2], Kang Yuejun[3], Vincent Chan[4,*], Chun Yang[2,*]

[1]School of Chemical annd Biomedical Engineering, Nanyang Technological University, 637459

[2]School of Mechanical and Aerospace Engineering, Nanyang Technological University, Singapore 639798

[3]Faculty of Materials and Energy, Southwest University, Chongqing, China 400715

[4]Department of Chemical Engineering, Khalifa University, Abu Dhabi Campus, United Arab Emirates 127788

Correspondence:

Vincent Chan, Department of Chemical Engineering, Khalifa University, Abu Dhabi Campus, United Arab Emirates 127788. **Email:** vincent.chan@kustar.ac.ae

Chun Yang, School of Mechanical and Aerospace Engineering, Nanyang Technological University, 50 Nanyang Avenue, Singapore 639798. **Email:** mcyang@ntu.edu.sg, **Fax:** (+65) 6791 - 1859

Keywords: Oil-in-water emulsions, DC biased AC electric field, Ion concentration polarization, Pre-concentration, Separation.

Abbreviations: O/W, oil-in-water; **PDMS,** polydimethylsiloxane; **DC,** direct current; **AC**, alternating current; **DI**, deionized; **ICP**, ion concentration plarization; **EDL,** electric double layer; **DEP**, dielectrophoresis; **EO**, electroosmosis; **EP**, electrophoresis; $\mathbf{F_e}$, electrokinetic vortex; **PAH**, poly(allylamine hydrochloride); **PSS**, poly(sodium 4-styrenesulfonte).

Abstract

A novel continuous flow microfluidic platform specifically designed for environmental monitoring of O/W emulsions during an aftermath of oil spills is reported herein. Ionized polycyclic aromatic hydrocarbons which are toxic are readily released from crude oil to the surrounding water phase through the smaller oil droplets with enhanced surface area. Hence, a multi-module microfluidic device is fabricated to (1) form ion enrichment zones in the water phase of O/W emulsions for the ease of detection and (2) to separate micron-sized oil droplets from the O/W emulsions. Fluorescein ions in the water phase, are used to simulate the presence of these toxic ions in the O/W emulsion. A DC-biased AC electric field is employed in both modules. In the first module, a nanoporous Nafion membrane is used for activating the concentration polarization effect on the fluorescein ions, resulting in the formation of stable ion enrichment zones in the water phase of the emulsion. A 35.6% amplification of the fluorescent signal is achieved in the ion enrichment zone; corresponding to 100% enrichment of the fluorescent dye concentration. In this module, the main inlet is split into two channels by using a Y-junction so that there are two outlets for the oil droplets. The second module located downstream of the first module consists of two oil droplet entrapment zones at two outlets. By swiching on the appropriate electrodes, either one of the two oil droplet entrapment zones can be activated and the droplets can be blocked in the corresponding outlet.

Introduction

Separation of water-soluble ions from oil-in-water emulsions (O/W) is of great importance for environmental monitoring of hazardous chemicals generated from oil spills. Water soluble ions such as ionized forms of polycyclic aromatic hydrocarbons (PAH) [1]

present in crude oil are harmful to the environment. In the aftermath of an oil spill from oil tankers, surfactants are generally used to break down the oil phase into small oil droplets with sizes less than or equal to70 μm [2], resulting in the formation of stable O/W emulsions. These smaller oil droplets with enhanced surface area to volume ratio readily release PAH to the surrounding environment. Hence, the detection of these water soluble ions such as PAH in O/W emulsions is important. But these O/W emulsion samples cannot be directly injected into standard analytical instrumentation such as gas chromatography [3], high-performance liquid chromatography [4], etc. for the detection of PAH ions. It is because the presence of oil in these multiphase O/W emulsions will lead to inaccurate result from conventional analytical measurement. As a result, novel methodology is needed for augmenting existing pre-concentration techniques such as ion concentration polarization [5, 6] (ICP), field amplified stacking [7], temperature gradient focusing [8], isoelectric focusing [9], isotachophoresis [10-12] , etc. for the detection of these ions in the complex multiphase emulsions which will be further followed by spectrophotometric [4] or electrochemical [13] detections.

Standard analytical instruments are also bulky and expensive and need highly trained personnel, which makes real-time field analysis difficult. Environmental monitoring [14-16] and detection [17] of targeted analytes using microfluidic devices is an important research area as it brings significant advantages such as portability for on-field analyses over traditional batch reactors. The development of fully automated and multi-functional microfluidic devices for continuous extraction and concentration of oil droplets will lower the sample volume consumptions, risk of contamination, need of sample transportation, etc. To simulate the complexity of the real-time O/W emulsions containing PAH ions in the water phase in our work, an emulsion of silicone oil droplets in deionized (DI) water containing solubilized

fluorescein sodium salt is used herein. It is noted that both phenolate ions and fluorescein ions are negatively charged when solubilized in water.

In this work, we introduce a novel design of micro-fluidic device with two modules known as Module I and II. In Module I, a nanoporous Nafion membrane is introduced for pre-concentrating the ions present in the water phase of O/W emulsion in a designated zone. The goal as mentioned above is achieved by using an electric-field induced ion concentration polarization (ICP) trapping scheme. This pre-concentration step may also be used in the identification of trace quantities of ions in O/W emulsions. This is because the formation of enriched ion concentration zones can increase the detection sensitivity of PAH ions in terms of stronger UV absorbance by using online fluorescence based detection techniques [18]. In Module II, an electrokinetic valve is incorporated for the separation of micron sized oil droplets from water by employing a Y-junction design with two outlets. Through activation of electric field, the passage of oil droplets is blocked in one of the two outlets. This unique approach is useful for the separation of micron-sized oil droplets from O/W emulsions by shutting off the flow of oil droplet in one of the two outlets.

Working principle

The novelty of this work stems on Module I which is based on the ion concentration polarization [5] (ICP) in O/W emulsion sample flow whereas Module II is an extension from our previous work [19]. ICP is an ion transport phenomenon and is observed when an electric potential is applied near the microfluidic and nanofluidic interface. The nanofluidic domain is provided by the nanoporous membrane which is connected to two larger sets of microfluidic channels: one is connected to an applied voltage; the other is connected to the ground. The pores

within the membrane act as nanochannels. Generally, common ion-selective membrane like Nafion which is negatively charged with sulfonic groups is used as the nanoporous membrane. When an electric field is applied, positively charged electric double layer (EDL) is generated within the negatively charged nanopores. As both nanopores and EDL have the same order of magnitude, overlapping [5] of the EDL within the nanopores takes place under the applied electric field. This leads to the accumulation of cations in the EDL and influences the ion fluxes at the junction where the Nafion is connected to the larger channel. Once the ICP process is stabilized, ion enrichment zones are induced in those regions. This phenomena has been utilized for a wide range of applications such as separation, concentration [5, 20-22], desalination[23, 24], mixing[25], etc of target analyte species.

Conventionally, single phase solutions with a direct current (DC) power supply were used for driving ICP. Due to the presence of oil droplets in water herein, it is observed that a DC voltage exerts an electroosmotic (EO) force on the droplets from the anode up to the Nafion membrane which is connected to the ground. Hence, there is no ion enrichment zone near the Nafion membrane. When a DC-bias is imposed to an alternating current (AC) [26] field, an ion enrichment zone is successfully generated near the Nafion membrane at the Y junction. The ion enrichment zone occurs because the net field maintains a steady electric potential for moving the anions towards the cations at the EDL of Nafion membrane. The module is also integrated with a Y junction for trapping the oil droplets in one of the two outlets and for selectively releasing the oil droplets from one of the two outlets.

A schematic diagram of the two modules as well as the layout of the overall device is shown in Fig. 1. The device has five electrodes: two of which are connected to the positive

terminal, V of the power supply. The remaining three electrodes: G1, G2 and G3, are connected to the ground. For inducing the effect of concentration polarization in Module I, electrodes V and G1 need to be turned on. As a result, ion enrichment zones are observed in the regions between AA` and the Nafion membrane as well as between BB` and Nafion membrane. Module II contains two electrodes connected to the ground, G2 and G3. When electrodes, V and G2, are turned on; the droplets no longer escapes from outlet 1 due to the oil entrapment zone along outlet 1. Similarly, when electrodes, V and G3, are turned on; the droplets no longer escapes from outlet 2 due to the oil entrapment zone along outlet 2. As long as the electrodes V and G1 are turned on, it is observed that the ions enrichment zones are formed in Module I regardless of the on/off status of the ground electrodes G2 and G3 connecting to the power supply.

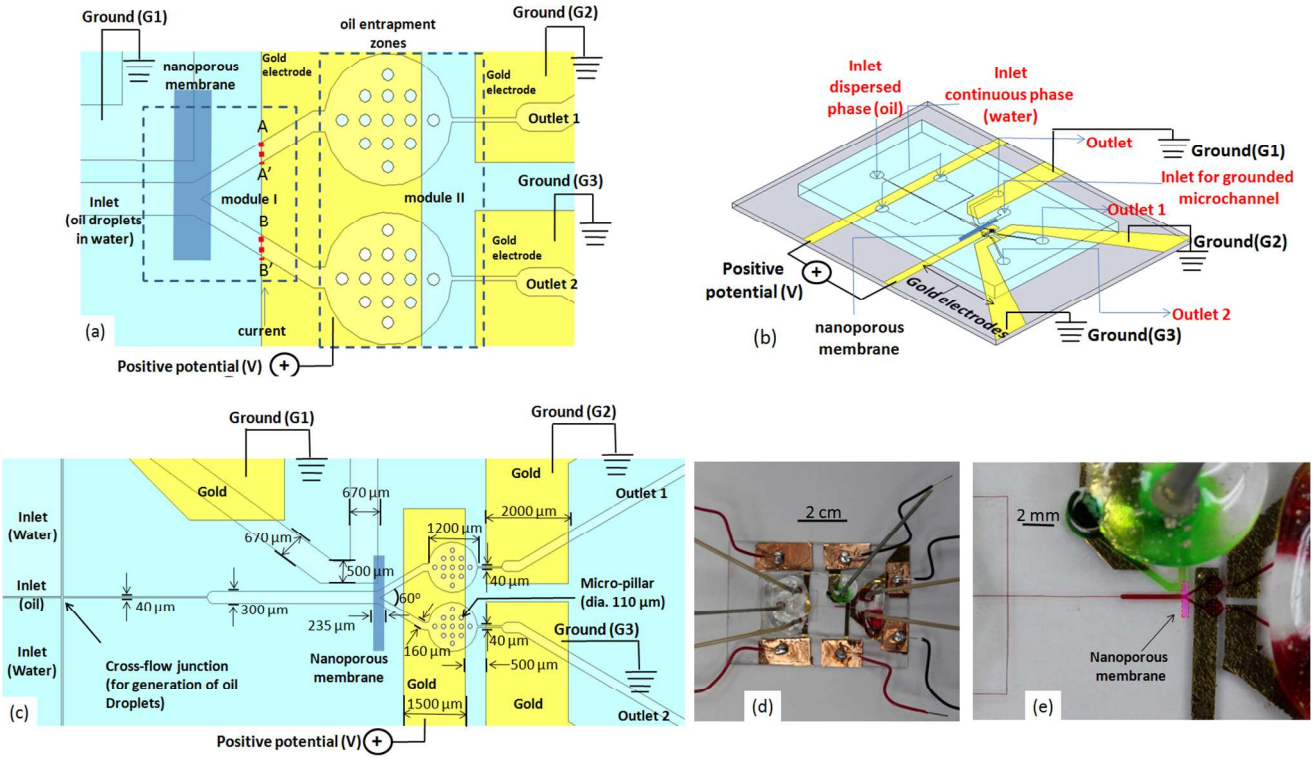

Fig.1 (a) Module I for ion preconcentration in the zone between AA` and Nafion as well as between BB` and Nafion, module II with the two trapping zones for oil droplets either along outlet I or outlet II. Electrodes designated as V are connected to the positive terminal of the power supply source and electrodes; G1, G2 and G3 are connected to the ground. (b) The overall layout of the microchip showing the inlets for dispersed phase, oil and continuous phase, water; nanoporous Nafion membrane and the gold electrodes over the PDMS-coated glass

substrate. (c) Detailed dimensions of the microchannels and electrode gaps. Height of the microchannel and micro-pillars is 40 microns and diameter of the micro-pillars in the two circular oil droplet entrapment zones is 110 microns. (d), (e) Photographs of the actual microfluidic device.

Experimental

Microchip Fabrication

The microfabrication process for the Nafion integrated gold electrode substrate is shown in Fig. 2. It is noted that the etching of gold in the final step involving the use of both acetone and scotch tape requires cautious work. First, a glass slide is spincoated with a 1:1 weight fraction of PDMS prepolymer (Dow Corning, Slygard 184) and hexane (Fisher Scientific) mixture at 500 rpm [27]. The PDMS prepolymer itself is first prepared by mixing PDMS curing agent with the PDMS base monomer in the 1:10 weight fraction. Nafion membrane (NR-212, DuPont Co.) is then placed over the top of the spincoated surface[22]. We place the substrate at room temperature so that the polymers reflow over the membrane. The substrate is again spincoated at 500 rpm with another layer of 1:1 weight fraction of PDMS prepolymer and hexane to form a completely flat surface and thereafter cured at 80 ^{o}C for 2 hours. This step of integration of Nafion membrane is followed by the fabrication of gold microelectrodes on the substrate. First, patterns of microelectrode are formed over the substrate by using AZ 9260 photoresist followed by UV exposure. Then an adhesion layer of chromium (~20 nm) followed by gold (~ 250 nm) is sputtered over the substrate. A lift-off process is then performed by using acetone and scotch tape to finally form the gold microelectrodes. The gap of 500 microns between the gold electrodes in Module II is etched manually with the tip of the BD insulin ultrafine needles (with an outer diameter of 336 microns). A PDMS block is then placed over the base substrate after plasma treatment. The height of the resulted microchannels is 40 microns. Finally, hydrophilization of the PDMS microchannels is done by layer-by-layer

deposition scheme of alternately charged polyelectrolyte solutions: poly(allylamine hydrochloride) (PAH) (Sigma) and negatively charged poly(sodium 4-styrenesulfonte) (PSS) by flushing it in the sequence of PAH-PSS-PAH-PSS[28] immediately after the plasma treatment.

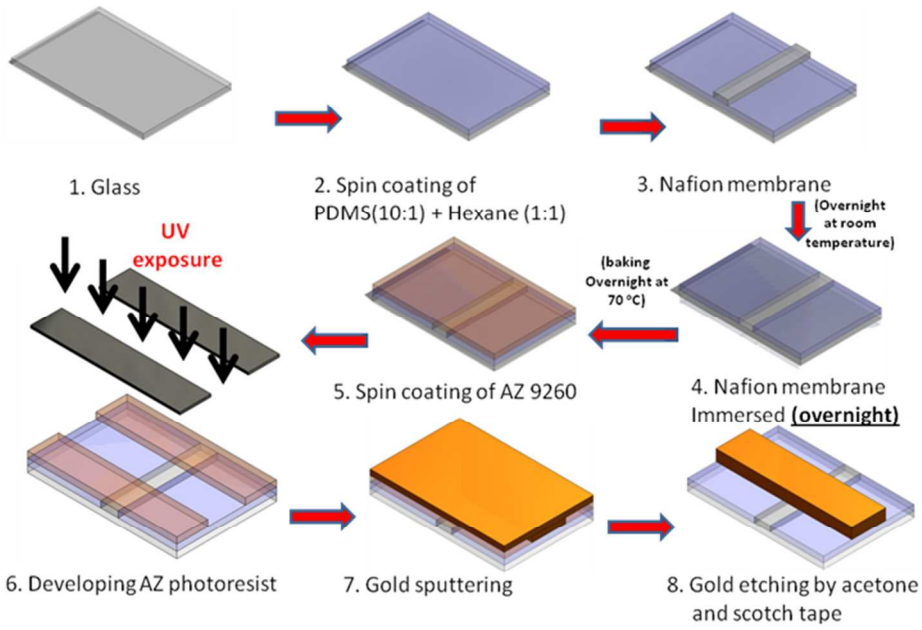

Fig.2 Schematic for the integration of the Nafion membrane into the base substrate and the photolithographic deposition and etching of gold electrodes on the same substrate.

Experimental Set up

Silicone oil (Sigma, Singapore) with viscosity of 50 cSt is used as the dispersed phase herein. The oil phase is then emulsified into discrete droplets in the presence of an aqueous and immiscible non-ionic surfactant known as Triton X-100 (Bio-Rad Laboratories) solution at the critical micelle concentration, which fills up the continuous and immiscible aqueous phase. The continuous phase also contains sodium fluorescent salt (Sigma) at 10 μM in concentration. A cross flow junction is applied for the emulsification of the dispersed phase consisting of silicone oil (50 cSt, density=960 kg/m3) into individual droplets [19].

Two syringe pumps (Longer) with 0.5 ml Hamilton glass syringes are used for pushing two immiscible fluids: the dispersed phase, oil and the continuous phase, water at 0.02 ml/hr and 0.1 ml/hr, respectively. A syringe pump (Longer) is also used at the two outlets, 1 and 2, in the withdrawal mode. There is a noticeable pressure drop in our device due to the complex geometry of the microfluidic channels. So to facilitate the flow of emulsion samples a suction pressure is applied at the outlet. The fluorescent imaging and the oil droplets separation at the bifurcation zone of the microchip is observed with an inverted microscope (Carl Zeiss, Germany) fitted with a mercury lamp. The microscope is also fitted with an objective lens (Carl Zeiss CP-Achromat 5x/0.12) and high-speed CMOS camera (Phantom Miro ex4). The fluorescent images are obtained at an exposure time of 0.099 seconds. A DC power supply (Model PS 350, Stanford Research systems, Inc.) is used to provide the DC field whereas a function generator (Agilent 33250A) connected with an amplifier (AVC 790 Series Power Amplifier) by a BNC cable is used to produce DC-biased AC field on the gold electrodes. The DC-bias AC signal is monitored with an oscilloscope (CombiScope, HM 1008-2).

Results and discussion

Module I: Ion concentration enrichment

In this module, ion pre-concentration in the water phase of oil-in-water emulsions is tested initially by using only a DC field as DC remains to be the popular choice for ICP so far. No ion enrichment zones are observed. The experimental observations are given in the supporting information. Afterwards, a positive DC biased AC field is investigated. Ion enrichment zones are successfully obtained when a positive DC biased AC field is applied. The experimental observations are shown in Fig. 3(a)-(d). The droplets at the cross-flow junction

[19] are generated using an external water phase flow rate at 0.1 ml/hr and an oil flow rate at 0.2 ml/hr. The electrokinetic flow induces a single rotating vortex [29]. A schematic of this vortex is shown in Fig. 3(f) and is denoted by F_e. The direction of the vortex is from the ground towards the anode. Under the influence of this vortex, the velocity of the droplets increases along both outlets, from the Nafion to AA` and from the Nafion to BB`. However, the velocity of the droplets decreases near the edges of anode due to the strong EOF force which is being exerted both from AA` and BB' towards the Nafion connected to the ground. This effect can be seen in Fig. 3(g) when the positive DC biased AC field is turned on. As we have used a Nafion which is a cation selective membrane, there will be a net accumulation of cations due to the overlap of the EDL within the nanopores of the membrane. To maintain the electroneutrality in the region, there will be a strong electrophoretic (EP) force exerted on the negatively charged fluorescein ions towards the cation saturated Nafion membrane. This will be further strengthened by the EOF force. This results in a net accumulation of anions, leading to the formation of ion enrichments zones near the Nafion membrane against the hydrodynamic force. This force is found to be strong enough to overcompensate the opposing DC biased AC electrokinetic flow vortex.

To calculate the fluorescent dye concentration enhancement, we plot the grey scale value in the ion enrichment zone before and at t=6 seconds after the electric field is applied. Fig. 3(h) shows the fluorescence intensity profile along the dashed yellow line in the inset images. There is lack of smoothness in the grey scale value of the fluorescence intensity profile before the electric field is turned on because of the background noise [28] which is mainly due to the hydrophilicity of the multiple polyelectrolyte layers at the PDMS microchannel walls. In the region where the enriched ion concentration is obtained; the average grey scale value of the

fluorescent intensity profile reaches 90 before the electric field is turned on and the grey scale reaches 122 after the electric field is turned on, we obtain a 35.6% amplification in the fluorescent signal for the ions in the water phase of the O/W emulsion which correlates to 100% enrichment of the dye concentration in the water phase of the O/W emulsion. This enrichment factor is similar to the values reported by other researchers [5, 20].

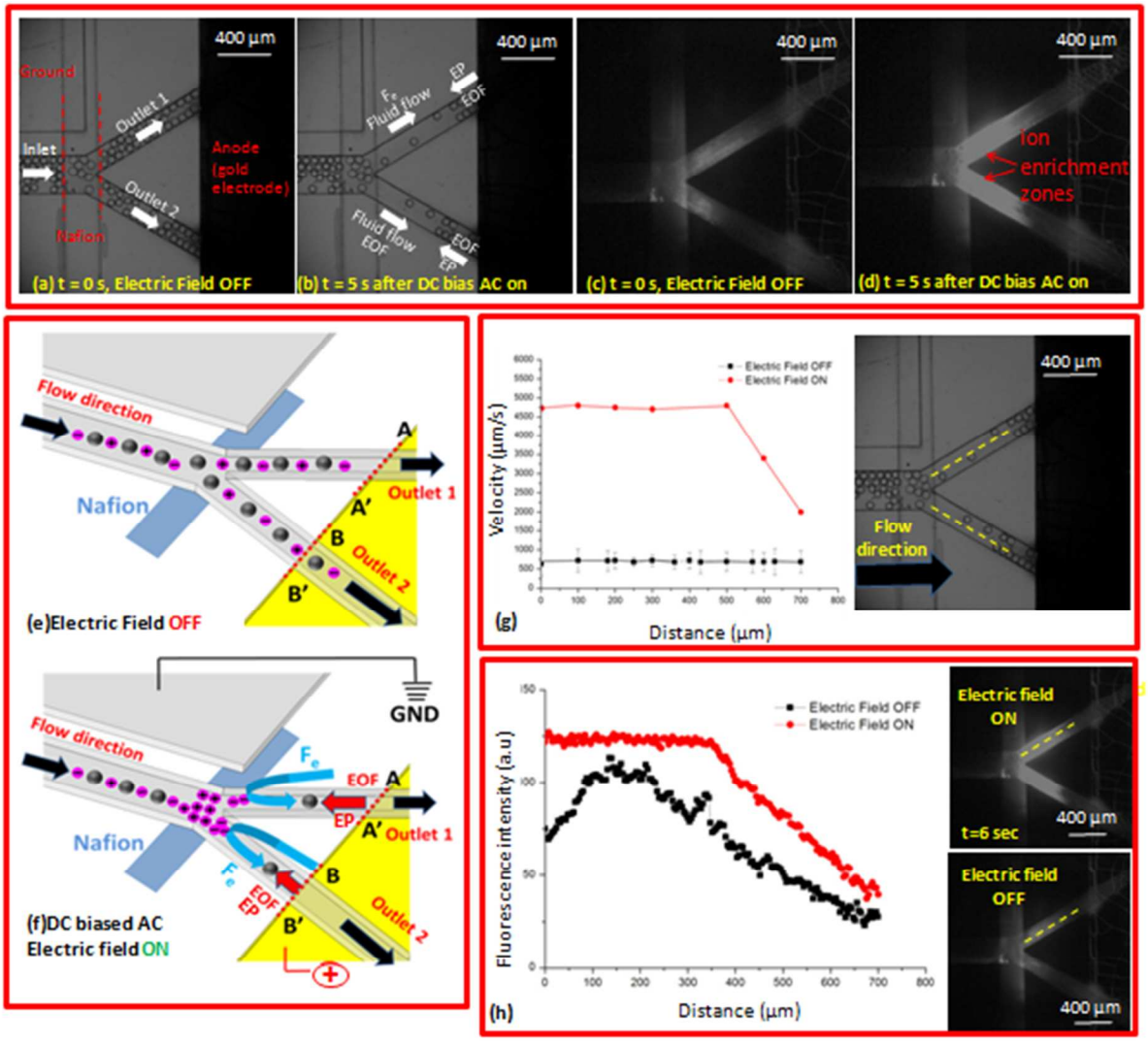

Fig.3 (a) the exit of oil droplets from the Y junction via outlets 1 and 2 without any electric field applied; (b)-(d): a DC biased AC electric field is on. (e)-(g): a positive DC biased AC field is on. (b) strong repulsion of droplets from the anode when the positive DC biased AC field of DC offset= 78 V and V_{p2p} =173 V at 100 Hz is applied. (c) fluorescein ions present in the water phase become visible when normal light is turned off and the mercury lamp is turned on. No electric field is applied; (d) enrichment zones of fluorescein ions observed when the positive DC biased AC field electric field is turned on. (e) Schematic illustration of the forces on the O/W emulsion with ions in the water phase when the electric field is off and (f) on. F_e denotes the

DC-biased AC electrokinetics flow vortex. (g) Average axial velocity of the droplets along the dashed yellow line (inset figure) before and after DC biased AC electric field is applied.(h) Fluorescence intensity along the dashed yellow line (inset figure) before and t= 6 seconds after the positive DC-biased AC electric field is applied.

Time sequential images of the gradual build-up of fluorescein ion concentration at the Nafion edge are shown in Fig. 4. An electric field of 78V + 173sin(2π(100 Hz)) is applied, and it is equivalent to an root mean squared voltage of 200V. As the fluorescein ions go past the Nafion membrane and reach the bifurcation of the Y-junction, they are subjected to two different EOF forces: one from AA' to the Nafion membrane along outlet 1 and the other from BB' to the Nafion membrane (connected to the ground) along outlet 2. A schematic illustration of the forces is shown in Fig. 3(f). However, the strength of the EO force is greater at BB' than AA' as it is closer to the voltage power source. Voltage strength decreases away from the source due to the electrical resistance of the substrate. This generates a stronger EO force from BB' to the Nafion membrane than that from AA' to the Nafion membrane, leading to faster build-up of fluorescein ions at the Nafion edge towards BB' from 0 to 0.4 seconds. Thereafter, ion concentration trapped in the region between the Nafion membrane edge and BB' exerts a repulsive Coulombic force to the incoming ions. Therefore an increase in the ion concentration between AA' and the Nafion membrane, is observed from 0 to 2.8 seconds after which a balance is reached between the hydrodynamic force and EO force. From 2.8 seconds onwards, the ion concentration along outlet 2 increases due to the combinatorial effect of the repulsive Coulombic force exerted by the higher ion concentration between AA' and Nafion membrane along outlet 1 to the incoming ions as well as the EO forces along both outlets,. Finally, at 5.2 seconds, steady ion enrichment zones are maintained along both outlets. Fig. 4(b) shows the growth in the ion concentration area along both outlets1 and 2 over time.

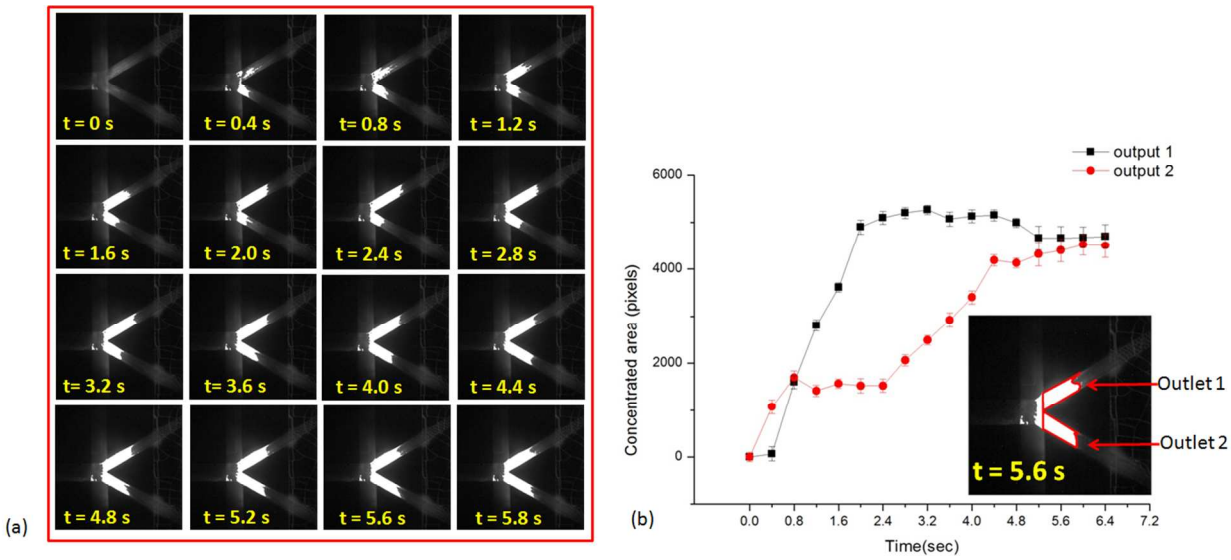

Fig.4 (a) Post-processed images (using ImageJ, an open source image processing software) showing the build-up of the ion enrichment zone near the Nafion membrane at the Y junction. Post-processing is performed by adjusting the threshold of the images and thereafter setting the brightness value of the altered images at 100. This step is necessary for highlighting the ion enrichment zones. (b) plot of the area of ion enrichment zone along both outlet 1 and output 2 over time, based on the area evaluation in (a) as shown in the inset figures.

Module II: Electrokinetic valve for the separation of oil droplets

This module consists of two outlets connected to the concentration polarization region in Module I via a Y junction. In the absence of electric field, there exists an equilibrium between the rate of incoming and outgoing droplets and the droplets exit through both outlets 1 and 2. For this module, we use an external water phase flow rate of 0.15 ml/hr while the oil phase flow rate is kept at 0.02 ml/hr. Fig. 5(b) shows the trapped oil droplets in outlet 1 when electrodes V and G2 are connected to the power supply [Fig. 1(b)]. The greater the flow rate of the fluids at the inlet, the higher the throughput of the device will be. In our previous work [19], the oil droplets were trapped at a much lower flow rate of 0.04 ml/hr. In our previous study, only an AC field is applied to generate two counter rotating vortices and to push the droplets away from the electrode gap [12]. In this study, a positive DC-biased AC field is applied to produce an

electrokinetic flow vortex directed from the ground towards the anode; which is acting against the incoming oil droplets, and hence aiding oil entrapment. Another factor is that that the external phase reported previously consists of DI water with a non-ionic surfactant, Triton X-100, while rapid generation of bubbles is observed in the presence of fluorescein ions at the ITO electrodes [12]. In this work, the gold electrodes, being a noble metal and chemically inert are more stable in the presence of ions inside our external water phase. The presence of fluorescein ions increases the difference in the polarizability between the non-polar oil droplets and the external water phase. Thus the strength of DEP force is amplified as the Clausius-Mossotti factor increases. An electric field of 78V +173sin(2π(100 Hz)) is the same as that for inducing the concentration polarization at the Y junction near the Nafion membrane in Module I. The applied frequency is kept at 100 Hz because the maximum entrapment efficiency is obtained at this particular frequency [12].

As shown in Fig. 5(b), the oil droplets at outlet 1 are trapped by connecting the electrodes V and G1 to the power supply. Alternately, we can also trap the droplets at outlet 2 and release the droplets via outlet 1. The use of micro-pillars is necessary in order to reduce the hydrodynamic force of the incoming oil droplets. By reducing the distance between the micro-pillars as well as by increasing the diameter of individual micro-pillars, the resistance against the incoming hydrodynamic pressure can be further increased. In our experiments, all micro-pillars have the same diameter of 110 μm.

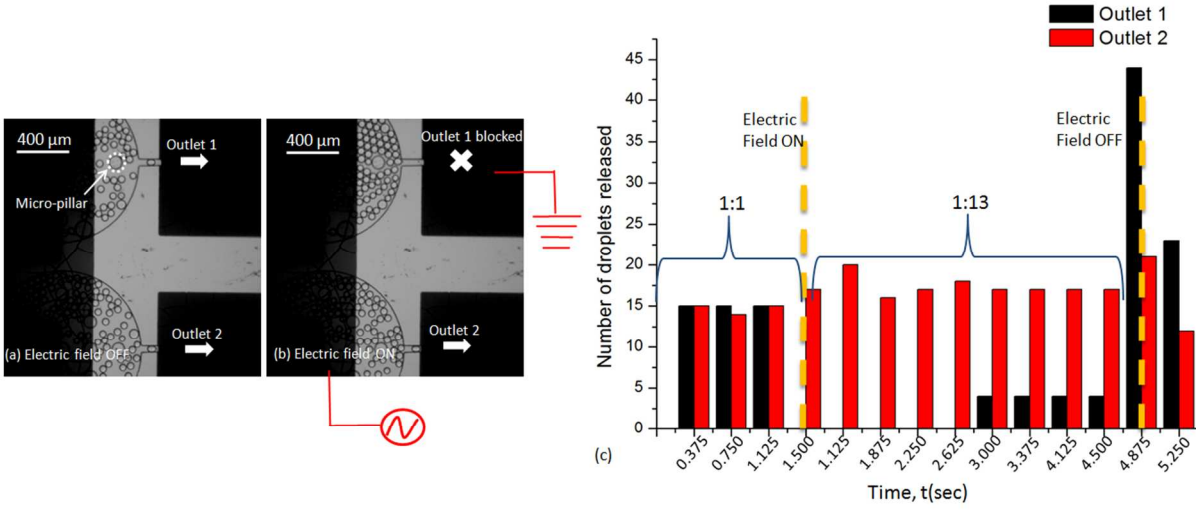

Fig.5 (a) Electric field is off and droplets exit at both outlet 1 and 2 (b) t= 2 seconds after an electric field of 78V +173sin(2π(100 Hz)) is applied. Trapping zone at outlet 1 is saturated with oil droplets (b). (c) Count of the total number of droplets escaping from outlet 1 and outlet 2 before and after electric field is applied. Electric field is turned on at 1.5 seconds and turned off at 4.875 seconds.

The significance of this module hinges on an electrokinetic valve for the separation of oil droplets from an O/W emulsion in a continuous flow reactor. As seen in Fig. 5(c), before the electric field is turned on, the total count of droplets released from outlet 1 and 2 are roughly the same. In the time interval when the electric field is turned on from t=1.5 sec to t=4.875 sec; the total number of droplets being released from outlet 1 is only 12 whereas 156 droplets escape from outlet 2. Although it is difficult to shut off the flow of oil droplet completely in one of the two outlets, it is possible to alter the oil droplets count escaping from the two outlets 1 and 2 from 1:1 to 1:13. After the electric field is turned off at t=4.875 sec, there is a sudden spike in the number of droplets released from outlet 1 as it is completely saturated with droplets [Fig.5 (b)]. In our design, the oil droplets are trapped to a certain extent until the trapping zone is saturated and the electrokinetic forces can no longer withstand the hydrodynamic pressure of the incoming fluids. However, by lowering the flow rate of the device and by using the stronger electric field, the trapping efficiency of the device can be further improved.

5.4 Summary

A microfluidic device for the analysis of O/W emulsions is presented herein for environmental monitoring. The platform may have important implications in the realization of ion pre-concentration techniques for studying complex O/W emulsion fluids. This device has two modules with the first one meant for inducing concentration enrichment of the ions present in the external water phase by using the ion concentration polarization effects and the second one meant for the separation of oil droplets from the O/W emulsion by using the electrokinetic phenomena. A Nafion membrane is embedded as a nanoporous junction for activating the concentration polarization effect. A positive DC-biased AC electric field instead of the conventional DC electric field is applied to enhance the concentration effect. Using the positive DC-biased AC electric field, a stable ion enrichment zone is observed after 6 seconds at both outlets of the Y-junction near the Nafion membrane and 35.6% amplification of the fluorescent signal in the ion enrichment zone is achieved. This result implies 100% enrichment of the fluorescent dye concentration in the water phase of the O/W emulsion. Moreover, this module is successfully integrated with an oil droplet separation unit using a Y-junction where the same electric field is used to alter the oil droplet ratio in the water phase from 1:1 to 1:13 at the two outlets.

Supporting information

A video is provided to schematically illustrate the two microfluidic modules and show the experimental processes of the two modules. Experimental images showing the effect of a pure DC field in module I are also provided in the supporting information.

D.D. gratefully acknowledges the postgraduate student scholarship from NEWRI, Singapore which is supported by Singapore National Research Foundation under its Environmental & Water Technologies Strategic Research Programme and administered by the Environment & Water Industry Programme Office (EWI) of the Public Utilities Board (PUB).

The authors have declared no conflict of interest.

References

[1] Mascarelli, A., *Nature* 2010, *467*, 22.
[2] Mendoza, W. G., Riemer, D. D., Zika, R. G., *Environmental Science: Processes & Impacts* 2013, *15*, 1017-1030.
[3] Fu, S., Fan, J., Hashi, Y., Chen, Z., *Talanta* 2012, *94*, 152-157.
[4] Oliferova, L., Statkus, M., Tsysin, G., Shpigun, O., Zolotov, Y., *Analytica Chimica Acta* 2005, *538*, 35-40.
[5] Pu, Q., Yun, J., Temkin, H., Liu, S., *Nano Letters* 2004, *4*, 1099-1103.
[6] Ko, S. H., Song, Y.-A., Kim, S. J., Kim, M., Han, J., Kang, K. H., *Lab on a Chip* 2012, *12*, 4472-4482.
[7] Jung, B., Bharadwaj, R., Santiago, J. G., *Electrophoresis* 2003, *24*, 3476-3483.
[8] Ge, Z.W., Wang, W., and Yang, C., *Lab on a Chip* 2011, *11*, 1396-1402.
[9] Cui, H., Horiuchi, K., Dutta, P., Ivory, C. F., *Analytical chemistry* 2005, *77*, 1303-1309.
[10] Bottenus, D., Jubery, T. Z., Ouyang, Y., Dong, W.-J., Dutta, P., Ivory, C. F., *Electrophoresis* 2011, *32*, 550-562.
[11] Bottenus, D., Hossan, M. R., Ouyang, Y., Dong, W.-J., Dutta, P., Ivory, C. F., *Lab on a Chip* 2011, *11*, 3793-3801.
[12] Bottenus, D., Jubery, T. Z., Ouyang, Y., Dong, W.-J., Dutta, P., Ivory, C. F., *Lab on a Chip* 2011, *11*, 890-898.
[13] Gunasingham, H., Tay, B. T., Ang, K. P., Koh, L. L., *Journal of Chromatography A* 1984, *285*, 103-114.
[14] Delattre, C., Allier, C. P., Fouillet, Y., Jary, D., Bottausci, F., Bouvier, D., Delapierre, G., Quinaud, M., Rival, A., Davoust, L., Peponnet, C., *Biosensors and Bioelectronics* 2012, *36*, 230-235.
[15] Das, D., Duraiswamy, S., Yi, Z., Chan, V., Yang, C., *Separation Science and Technology* 15 Jan, 2015, *50*, 7.
[16] Marle, L., Greenway, G. M., *TrAC Trends in Analytical Chemistry* 2005, *24*, 795-802.
[17] Soares, R. R. G., Novo, P., Azevedo, A. M., Fernandes, P., Aires-Barros, M. R., Chu, V., Conde, J. P., *Lab on a Chip* 2014, *14*, 4284-4294.
[18] Kuijt, J., García-Ruiz, C., Stroomberg, G. J., Marina, M. L., Ariese, F., Brinkman, U. A. T., Gooijer, C., *Journal of Chromatography A* 2001, *907*, 291-299.
[19] Das, D., Yan, Z., Menon, N. V., Kang, Y., Chan, V., Yang, C., *RSC Advances* 2015, *5*, 70197-70203.
[20] Phan, D.-T., Shaegh, S. A. M., Yang, C., Nguyen, N.-T., *Sensors and Actuators B: Chemical* 2016, *222*, 735-740.
[21] Lee, J. H., Song, Y.-A., Han, J., *Lab on a Chip* 2008, *8*, 596-601.
[22] Phan, D.-T., Yang, C., Nguyen, N.-T., *RSC Advances* 2015, *5*, 44336-44341.
[23] Kim, S. J., Ko, S. H., Kang, K. H., Han, J., *Nat Nano* 2010, *5*, 297-301.
[24] MacDonald, B. D., Gong, M. M., Zhang, P., Sinton, D., *Lab on a Chip* 2014, *14*, 681-685.
[25] Jännig, O., Nguyen, N.-T., *Microfluidics and Nanofluidics* 2011, *10*, 513-519.

[26] Ng, W. Y., Goh, S., Lam, Y. C., Yang, C., Rodriguez, I., *Lab on a Chip* 2009, *9*, 802-809.
[27] Chen, W., Lam, R. H. W., Fu, J., *Lab on a Chip* 2012, *12*, 391-395.
[28] Bauer, W.-A. C., Fischlechner, M., Abell, C., Huck, W. T. S., *Lab on a Chip* 2010, *10*, 1814-1819.
[29] Ng, W. Y., Ramos, A., Lam, Y. C., Mahendra Wijaya, I. P., Rodriguez, I., *Lab on a Chip* 2011, *11*, 4241-4247.